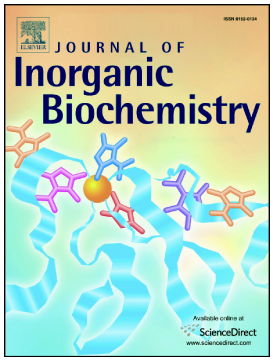

New ruthenium compounds bearing semicarbazone 2-formylopyridine moiety: Playing with auxiliary ligands for tuning the mechanism of biological activity

Michał Łomzik, Olga Mazuryk, Dorota Rutkowska-Zbik, Grażyna Stochel, Philippe C. Gros, Małgorzata Brindell

PII: S0162-0134(17)30314-8
DOI: doi: 10.1016/j.jinorgbio.2017.07.006
Reference: JIB 10253

To appear in: *Journal of Inorganic Biochemistry*

Received date: 3 May 2017
Revised date: 4 July 2017
Accepted date: 9 July 2017

Please cite this article as: Michał Łomzik, Olga Mazuryk, Dorota Rutkowska-Zbik, Grażyna Stochel, Philippe C. Gros, Małgorzata Brindell , New ruthenium compounds bearing semicarbazone 2-formylopyridine moiety: Playing with auxiliary ligands for tuning the mechanism of biological activity, *Journal of Inorganic Biochemistry* (2017), doi: 10.1016/j.jinorgbio.2017.07.006

New Ruthenium Compounds bearing Semicarbazone 2-Formylopyridine Moiety: Playing with Auxiliary Ligands for Tuning the Mechanism of Biological Activity

Michał Łomzik,[#[a],[b]] Olga Mazuryk,[#[a]] Dorota Rutkowska-Zbik,[[c]] Grażyna Stochel, [[a]] Philippe C. Gros,* [[b]] and Małgorzata Brindell*[[a]]

[a] Department of Inorganic Chemistry, Faculty of Chemistry, Jagiellonian University Ingardena 3, 30-060 Krakow, Poland. brindell@chemia.uj.edu.pl

[b] Université de Lorraine, CNRS, UMR SRSMC, HecRIn, Boulevard des Aiguillettes Vandoeuvre-Lès-Nancy, France. philippe.gros@univ-lorraine.fr

[c] Jerzy Haber Institute of Catalysis and Surface Chemistry, Polish Academy of Sciences, Niezapominajek 8, 30-239 Krakow, Poland.

[#] both authors contributed equally to this work

* corresponding authors: P.G. : email: philippe.gros@univ-lorraine.fr, phone: +33383684979 ; M. B. : email: brindell@chemia.uj.edu.pl, phone: +48126632221.

Keywords ruthenium, polypyridine**,** semicarbazone, anticancer activity, apoptosis, auxiliary ligands

Abstract

Two ruthenium(II) complexes **Ru1** and **Ru2** bearing as a one ligand 2,2'-bipyridine substituted by a semicarbazone 2-formylopyridine moiety (**bpySC:** 5-(4-{4'-methyl-[2,2'-bipyridine]-4-yl}but-1-yn-1-yl)pyridine-2-carbaldehyde semicarbazone) and as the others 2,2'-bipyridine (bpy) and 4,7-diphenyl-1,10-phenanthroline (dip), respectively, as auxiliary ligands have been prepared. Their biological activity has been studied on murine colon carcinoma (CT26) and human lung adenocarcinoma (A549) cell lines. The anti-proliferative activity was dependent on the presence of bpy or dip in the complex, with one order of magnitude higher cytotoxicity for **Ru2** (dip ligands). **Ru1** (bpy ligands) exhibited a distinct increase in cytotoxicity going from 24 to 72 h of incubation with cells as was not observed for **Ru2**. Even though both studied compounds were powerful apoptosis inducing agents, the mechanism of their action was entirely different. **Ru1**-incubated A549 cells showed a notable increase in cells number in the S-phase of the cell cycle, with concomitant decrease in the G2/M phase, while **Ru2** promoted a cell accumulation in the G0/G1 phase. In contrast, **Ru1** induced marginal oxidative stress in A549 cell lines even upon increasing the incubation time. Even though **Ru1** preferably accumulated in lysosomes it triggered the apoptotic cellular death via an intrinsic mitochondrial pathway. **Ru1**-incubated A549 cells showed swelling and enlarging of the mitochondria. It was not observed in case of **Ru2** for which mitochondria and endoplasmic reticulum were found as primarily localization site. Despite this the apoptosis induced by **Ru2** was caspase-independent. All these findings point to a pronounced role of auxiliary ligands in tuning the mode of biological activity.

1. Introduction

One of the most important issues in the field of medicinal inorganic chemistry concerns the discovery of more effective and safer anticancer drugs. Many of the currently studied metallodrugs are designed to be prodrugs and selectively activated in the cancer tissue. However, a major advantage of this strategy can also be its main weakness, since several possible active molecules are produced and start to interact with biomolecules in the human body. Investigation of all these interactions is very challenging and is still the focus of many studies. Because of this, the perspective about designing new anti-cancer drugs slowly shifted [1], and an increased attention is paid to ruthenium compounds inert to substitution mainly those with polypyridyl ligands. Their electronic and structural properties can be tuned easily by the selection of appropriate ligands giving rise to the formation of versatile compounds which might be designed either for therapeutic and/or optical imaging purpose.

The design of potential drugs based on organic compounds usually involves the modification of the lead structure in respect to the site of action, or otherwise new compounds are formed based on the known molecular targets (e.g. receptor proteins or enzymes) [2]. Even though many active ruthenium-based compounds have been discovered, their biological activity mechanism remains unclear and their targets still unidentified. The lack of this knowledge hampers rational design of new anticancer agents based on these complexes. A new approach recently developed, is to design compounds where one or more polypyridyl ligands around ruthenium center are modified by anchoring an organic molecule with a known biological target or mechanism of action. The choice of the organic targeting molecule is critical since it can have various functions such as *i*) tuning the lipophilic character of the whole Ru complex for specific subcellular accumulation (mitochondria, reticulum endoplasmic, nucleus, lysosome) [3, 4]; *ii*) targeting the specific

receptors, enzymes or cellular processes [5, 6]; *iii*) oxygen-dependent accumulation in cells [7, 8]; *iv*) creating synergistic effects between the biologically active ligand systems and the metal centre; *v*) tuning the photophysical/photochemical properties for an appropriate light activation (photodynamic and photoactivated therapy) [9, 10]; *vi*) combining therapy and diagnosis (theranostics) [11] and others.

In this context, we have designed two new ruthenium(II) polypyridyl complexes in which one bipyridyl ligand is modified by a semicarbazone 2-formylopyridine (Scheme 1). α-N-heterocyclic (thio)semicarbazones and their metal complexes are known as anticancer agents [12-14] therefore combining such moiety with Ru(II) polypyridyl complexes might bring additional benefits towards their anticancer activity. The chosen semicarbazone is a structural analogue of 3-aminopyridine-2-carboxyaldehyde thiosemicarbazone, which is currently clinically tested as an anticancer drug (Triapine®) [15, 16]. The anticancer activity of the Triapine® arises from its ability to inhibit the action of ribonucleotide reductase (RR) [17]. The catalytically active centre of RR comprises a tyrosyl radical stabilized with two iron ions which might be a target for Triapine® having good metal chelating properties [18]. Ribonucleotide reductase is required for DNA synthesis since it catalyses the reduction of ribonucleotides into deoxyribonucleotides. Consequently the inhibition of this enzyme interrupts cell proliferation. To take an advantage of its chelating properties, semicarbazone 2-formylopyridine moiety was kept away from Ru centre by a spacer based on an alkyne chain (Scheme 1). 2,2'-bipyridine (bpy) and 4,7-diphenyl-1,10-phenanthroline (dip) were chosen as auxiliary ligands to evaluate the impact of their diverse lipophilic character and size on the biological activity. The synthesis, photophysical properties and biological evaluation on two cancer cell lines: murine colon carcinoma (CT26) and human lung adenocarcinoma (A549) of the **Ru1** and **Ru2** complexes are reported. Their cytotoxicity,

cellular distribution, induction of apoptosis, effect on cell-cycles, mitochondria potential, intracellular calcium concentration as well as reactive oxygen production (ROS) are discussed in relation to the parent ruthenium(II) complexes ($[Ru(bpy)_3]^{2+}$ and $[Ru(dip)_2(bpy)]^{2+}$) to understand their mechanism of action. Our results prove that the choice of the auxiliary ligands might have a predominate effect on the mode of action of ruthenium complexes having one ligand modified with biologically active organic substituent.

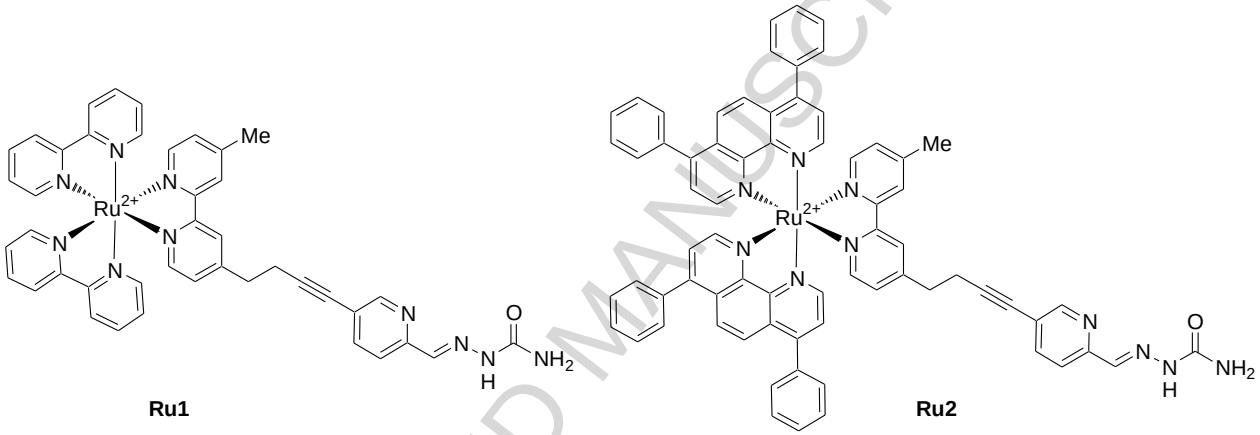

Scheme 1. Ruthenium compounds studied in this work.

2. Materials and methods

2.1. Synthetic procedures

All solvents were at analytical grade and were used without further purification. DMF was stirred over calcium hydride for 12 h, filtrated and distilled from over potassium carbonate [19]. Diisopropylamine was distilled over NaH and stored under argon [19]. Reagents were purchased from Sigma-Aldrich (ruthenium(III) chloride, *n*-butyllithium solution in hexanes, isopropylmagnesium solution in THF, 2,2'-bipyridyl, 4,7-diphenyl-1,10-phenantroline), Alfa

aesar (5-bromo-2-iodopyridine, semicarbazide hydrochloride, 3-(trimethylsilyl)propagyl bromide) concentration of n-butyllithium solution was determined by titration of diphenylacetic acid in dry THF [20].

2.1.1. Synthesis of 4-(3-(trimethylsilyl)prop-2-yn-1-yl)-4'-methyl-2,2'-bipyridyl (2). To a solution of freshly distilled diisopropylamine (0.19 mL, 1.3 mmol) in anhydrous THF (5 mL) under argon conditions at -78°C, a solution of n-butyllithium in hexane (0.75 mL, 1.2 mmol) was added dropwise. The solution was stirred for 30 minutes at -78°C and then warmed up to 0°C. A solution of 4,4'-dimethyl-2,2'-bipyridine (1) (0.184 g, 1 mmol) in dry THF (10 mL) was then added. After 2 h, 3-(trimethylsilyl)propagyl bromide (0.25 mL, 1.5 mmol) was added rapidly. After another hour, the mixture was warmed to room temperature and quenched with water (30 mL). The organic phase was extracted with diethyl ether (3x20 mL) and the combined organic layers were washed twice with brine and dried over magnesium sulphate. The solvent was removed under reduced pressure to give the pure product **2** (0.276 g, 92%). **2** was found too instable to be stored and was involved immediately in the next stage of the synthesis. ^{1}H NMR (400 MHz, $CDCl_3$): δ: 0.11 (s, 9H), 2.44 (s, 3H), 2.58 (t, *J*=7.2Hz, 2H), 2.91 (t, *J*=7.2 Hz, 2H), 7.12-7.14 (m, 1H), 7.18 (dd, *J*=4.8 and 1.6 Hz, 1H), 8.22 (s, 1H), 8.28 (s, 1H), 8.52 (d, *J*=5.2 Hz, 1H), 8.58 (d, *J*=4.8 Hz, 1H) ppm (Fig. S4). ^{13}C NMR (100 MHz, $CDCl_3$): (ppm): -0.01, 21.05, 21.19, 34.40, 86.16, 105.52, 121.40, 121.98, 124.03, 124.68, 148.11, 148.95, 148.99, 150.34, 155.94, 156.27 ppm (Fig. S5).

2.1.2. Synthesis of 4-(prop-2-yn-1-yl)-4'-methyl-2,2'-bipyridyl (3). To a solution of **2** (0.276 g, 0.9 mmol) in methanol (5 mL) was added potassium carbonate (0.205 g, 1.5 mmol). The mixture

was heated under argon at 50ºC for 2 h. After this time, the reaction was cooled down to 0°C, neutralized with 2M HCl and extracted with diethyl ether (3x30 mL). The combined organic layers were washed twice with brine and dried over magnesium sulphate. The solvent was removed under reduced pressure to give the pure product as a brown solid (0.150 g, 72%). ^{1}H NMR (400 MHz, $CDCl_3$): d 1.99 (t, *J* = 2.6 Hz, 1H), 2.44 (s, 3H), 2.54 (td, *J* =7.4 and 2.6 Hz, 2H), 2.94 (t, *J* = 7.4 Hz, 2H), 7.13 (d, *J*=4.8 Hz, 1H), 7.20 (dd, *J* =5.0 and 1.8 Hz, 1H), 8.23 (d, , *J* =0.8 Hz, 1H), 8.26 (d, *J* =0.8 Hz, 1H), 8.52 (d, *J*=5Hz, 1H), 8.58 (d, J=5Hz, 1H) ppm (Fig. S6). ^{13}C NMR (100 MHz, $CDCl_3$): d 20.41, 21.12, 34.50, 68.87, 83.79, 120.71, 121.63, 124.04, 125.02, 147.99, 148.33, 148.90, 151.03, 155.89, 156.32 ppm. [HRMS – ESI] Calculated for $C_{15}H_{14}N_2$ m/z : 223.1230 ($M+H^+$), Found: m/z = 223.1239 ($M+H^+$).

2.1.3. Synthesis of 5-bromo-2-formylpyridine (5) [21]. 5-bromo-2-formylpyridine was synthesized modifying the procedure described by Song et al. [21]. To a solution of 5-bromo-2-iodopyridine (**4**) (0.586 g, 2 mmol) in anhydrous THF (10 mL) under argon conditions at -10°C, a solution of isopropylmagnesium chloride (1.5 mL, 2.17 mmol) was added dropwise. After 2 h, dry DMF (0.4 mL, 5.16 mmol) was added rapidly. The mixture was kept at -10°C for another hour and then warmed up to room temperature over 2 h. The reaction was quenched with a saturated aqueous solution of NH_4Cl (20 mL) and extracted with diethyl ether (3x25 mL). The combined organic layers were washed twice with brine and dried over magnesium sulphate. The solvent was removed under reduced pressure to give pure product as light yellow solid (0.306 g, 80%). ^{1}H NMR (200 MHz, $CDCl_3$): δ 7.84 (dd, *J* = 8.2 and 0.8 Hz, 1H), 8.02 (ddd, *J* = 8.2, 2.2 and 0.8 Hz, 1H), 8.85 (d, *J*=2 Hz, 1H), 10.04 (d, *J*=0.8 Hz, 1H) ppm.

2.1.4. Synthesis of 2-[(5-bromopyridin-2-yl)methylidene]hydrazinecarboxamide (6). To a suspension of semicarbazide hydrochloride (0.149 g, 1.3 mmol) in anhydrous ethanol (3 mL), a solution of **5** (0.230 g, 1.2 mmol) in ethanol (9 mL) was added. The mixture was refluxed over 3 h and cooled down to 0°C. The solid was filtrated, washed twice with cold, anhydrous ethanol, once with diethyl ether and dried in vacuum to give the pure product as light cream powder (0.300 g, 99%). ^{1}H NMR (400MHz, DMSO-d_6) δ 7.02 (brs, 2H), 7.86 (s, 1H), 8.10 (dd, *J* = 8.0 and 1.6 Hz, 1H), 8.15 (d, *J* = 8.0 Hz, 1H), 8.67 (d, *J* = 1.6 Hz, 1H), 10.63 (s, 1H) ppm (Fig. S7). ^{13}CNMR (100MHz, DMSO-d_6): 119.70, 121.57, 137.78, 139.73, 149.26, 152.25, 156.29 ppm (Fig. S8). [HRMS-ESI]: Calculated for $C_7H_7N_4OBr$: m/z 264.9701 ($M+Na^+$) Found 264.9692 ($M+Na^+$).

2.1.5. Synthesis of 5-(4-{4'-methyl-[2,2'-bipyridine]-4-yl}but-1-yn-1-yl)pyridine-2-carbaldehyde semicarbazone (bpySC). To a solution of **3** (0.170 g, 0.75 mmol) in acetonitrile (6 mL), copper (I) iodide (0.05 g, 30 mol%) and Tetrakis(triphenylphosphine)palladium(0) (0.045 g, 5 mol%) were added under argon conditions. Diisopropylamine (6 mL) was added and the mixture was stirred for 15 min. After that, a suspension of **6** (0.210 g, 0.9 mmol) in methanol (1 mL) was added. The mixture was refluxed for 18 hours. Concentrated ammonia (1 mL) was added to the brown suspension and the mixture was filtrated through Celite (followed by 70 mL of acetonitrile). The solvent was removed under reduced pressure and the residue was dissolved in dichloromethane/concentrated ammonia mixture. The organic phase was separated, washed twice with concentrated ammonia (till all copper was removed), once with brine and dried over magnesium sulfate. The solvent was removed under reduced pressure to give the crude product which was dissolved in chloroform (15 mL) and treated with cyclohexane (60 mL). The mixture

was kept at 4°C (fridge) and crystals were filtrated, washed with cyclohexane and dried under vacuum to give the pure product as a white solid (0.132 g, 45%). ^{1}H NMR (600 MHz, $CDCl_3$): d 2.45 (s, 3H), 2.84 (t, *J* =7 Hz, 2H), 3.03 (t, *J* = 7 Hz, 2H), 7.14 (dd, *J* =16.2 and 4.8 Hz, 2H), 7.64-7.77 (m, 3H), 8.25 (s, 1H), 8.38 (s, 2H), 8.53-8.63 (m, 3H) ppm (Fig. S9). ^{13}C NMR (150 MHz, $CDCl_3$) d 20.67, 21.22, 34.17, 78.86, 93.77, 119.41, 120.83, 121.33, 122.04, 123.89, 124.83, 138.90, 141.49, 148.23, 148.95, 149.18, 150.04, 151.14, 152.11, 155.79, 156.38, 156.79 ppm (Fig. S10). [HRMS-ESI]: Calculated for $C_{22}H_{20}N_6O$ m/z 385.1771 ($M+H^+$) Found 385.1771 m/z ($M+H^+$).

2.1.6. General procedure for synthesis of cis-Ru(NN)$_2$Cl$_2$. Ruthenium(III) chloride trihydrate (0.262 g, 1 mmol), the ligand (2,2'-bipyridine or 4,7-diphenyl-1,10-phenantroline) (2 mmol) and 2 drops of N-ethylmorpholine were dissolved in degassed N,N-dimethylformamide (10 mL) under argon conditions. The mixture was put into a microwave reactor for 30 min (250W, 160ºC). The solvent was then removed under reduced pressure to c.a. 1 mL and acetone (20 mL) was added. After 24h at -20ºC, the dark solid obtained was filtrated and washed with cold acetone, twice with diethyl ether and dried under vacuum. The crude product was finally purified by flash chromatography (neutral Al_2O_3, dichloromethane/methanol (5/95)) to give the pure product.

2.1.6. 1. *cis*-Ru(bpy)$_2$Cl$_2$ (8) [22]. 8 was obtained using 2,2'-bipyridine as ligand (0.181 g, 38%). ^{1}H NMR (200 MHz, DMSO-d_6): δ 7.11 (t, *J* =8Hz, 2H), 7.51 (d, *J*=5.2Hz, 2H), 7.69 (t, 2H, J=8Hz), 7.78 (t, *J* =7Hz, 2H), 8.08 (t, *J* =8Hz, 2H), 8.48 (d, *J* =8Hz, 2H), 8.64 (d, *J* =8Hz, 2H), 9.97 (d, *J*=5Hz, 2H) ppm. [HRMS-ESI]: Calculated for $C_{20}H_{16}N_4RuCl_2$: m/z 483.9784 m/z (M+) Found 483.9791 (M+).

2.1.6.2. *cis*-Ru(dip)$_2$Cl$_2$ (9) [23]. 9 was obtained using 4,7-diphenyl-1,10-phenantroline as ligand (0.460 g, 55%). ^{1}H NMR (600 MHz, DMSO-d_6): δ 7.45-7.65 (m, 2H), 7.70 (t, *J* =7.8Hz, 4H), 7.81 (d, *J* =7.2Hz, 4H), 7.97 (d, *J* =9Hz, 2H), 8.25 (s, 1H), 8.27 (s, 1H) ppm**.** [HRMS-ESI]: Calculated for $C_{48}H_{32}N_4RuCl_2$: m/z 859.0929 m/z (M+Na$^+$) Found 859.0949 (M+Na$^+$).

2.1.6.3. Synthesis of [Ru(bpy)$_2$(bpySC)]Cl$_2$ (Ru1). bpySC (0.023 g, 0.060 mmol) was dissolved in absolute ethanol (5 mL) under argon conditions. A solution of *cis*-Ru(bpy)$_2$Cl$_2$(8) (0.023 g, 0.048 mmol) in absolute ethanol (5 mL) was finally added. The dark violet mixture was refluxed under argon for 16 h. After that, the solvent was removed under reduced pressure the residue was dissolved in water (1 mL) and filtrated. The pure product was obtained after crystallization from water as dark red crystals (0.033 g, 80%). ^{1}H NMR (600 MHz, CD_3CN): δ 2.51 (s, 3H), 2.91 (t, *J*=6 Hz, 2H), 2.95 (t, *J*=6 Hz, 2H), 7.19 (s, 1H), 7.33-7.40 (m, 6H), 7.46 (d, *J*=7.8 Hz, 1H), 7.51 (d, *J*=6 Hz, 1H), 7.61 (d, *J*=6 Hz, 1H), 7.71-7.74 (m, 6H), 7.80 (t, *J*=7.8 Hz, 1H), 8.03-8.07 (m, 4H), 8.13 (s, 1H), 8.25 (d, *J*=6 Hz, 1H), 8.54-8.66 (m, 8H) ppm (Fig. S11). [HRMS] Calculated for $C_{42}H_{36}N_{10}ORu$: m/z 399.1052 (M$^+$), Found 399.1058, (M$^+$) Anal. Calc. for $C_{42}H_{36}N_{10}ORu$: C (58.1%), H (4.2%), N (16.1%), Found: C (58.2%), H (4.4%), N (16.1%).

2.1.6. 4. Synthesis of [Ru(dip)$_2$(bpySC)]Cl$_2$ (Ru2). To a solution of **9** (0.019 g, 0.023 mmol) in absolute ethanol (10 mL) under argon conditions, was added a solution of **bpySC** (0.010 g, 0.026 mmol) in absolute ethanol (5 mL). The mixture was refluxed for 22 h. After that time the solvent was removed under reduced pressure. The crude product was dissolved in dichloromethane and purified by flash chromatography (Al_2O_3 neutral, dichloromethane/Methanol(5/95 to 10/90 gradient) to give the pure product with yield (0.013 g, 47%). ^{1}H NMR (600 MHz, CD_3CN) δ 2.55 (s, 3H), 2.95 (t, *J* =6 Hz, 2H), 3.13 (t, *J*=6 Hz, 2H), 7.04 (s, 1H), 7.22 (d, *J*=6 Hz, 1H), 7.37 (dd, *J*=15.6 Hz, 6 Hz, 2H), 7.57-7.63 (m, 20H), 7.67 (d, *J*=5.4 Hz, 2H), 7.73 (dd, *J*=5.4 and 2.4 Hz,

2H), 7.79 (t, *J*=5.4 Hz, 1H), 8.13-8.20 (m, 6H), 8.23 (d, *J*=5.4 Hz, 1H), 8.26 (d, *J*=5.4 Hz, 1H), 8.33 (d, J=5.4 and 3.6 Hz, 1H), 8.80 (d, J=12.6 Hz, 1H), 8.90 (d, J=12.6 Hz, 1H) ppm (Fig. S12). [HRMS]: m/z: Calculated for $C_{70}H_{52}N_{10}ORu$: m/z 575.1679 (M^+), Found 575.1658 (M^+).

2.2. Spectroscopy measurements

UV-Vis absorption spectra of ruthenium complexes were recorded at 25ºC in water using Perkin Elmer Lambda 35 spectrophotometer. Luminescence measurements were registered on Perkin Elmer LS55 spectrofluorimeter in the range 480 - 900 nm upon excitation at the maximum of charge transfer band for each ruthenium complex. The average of three scans was subjected to smoothing. For the determination of the quantum yield of luminescence (Φ), aqueous solutions of $[Ru(bpy)_3]^{2+}$ with a small amount of DMSO (<0.008% v/v) were used as standards (Φ = 0.028 [24] and 0.042 [25] for air-equilibrated and deoxygenated conditions, respectively). The spectra for the ruthenium complexes were recorded at a concentration that had an absorbance less than 0.05 units at the excitation wavelength. The quantum yield was calculated according to the following equation:[26]

$$\boldsymbol{\Phi = \Phi_{ref} \times [A_{ref}/A] \times [I/I_{ref}] \times [n^2/n_{ref}^2]}$$

where ***I*** is the integrated luminescence intensity, ***A*** is the optical density, and ***n*** is the refractive index, ***ref*** refers to the values for the reference. The mean value was calculated from a minimum of three independent experiments.

Luminescence lifetime experiments were performed at room temperature using Fluorolog-3 Horiba Jobin Yvon with single photon counting technique. The excitation wavelength was fixed at 464 nm (NanoLED diode) and average luminescence lifetime was measured at emission maximum. The instrument response functions were measured using a light scattering solution of Ludox (colloidal silica, Sigma-Aldrich). The DAS6 software (HORIBA Scientific) was used for

deconvolution of the obtained decays and for calculation of the lifetime values. Two or three exponential fit were chosen based on χ^2 parameter (the goodness of fit evaluation). A single-exponential fit was found to be an optimal description of the obtained results for the ruthenium compounds.

2.3. Computational characterization

To obtain ground state geometries and electronic structures of Ru1 and Ru2 Density Functional Theory (DFT) was applied using hybrid B3LYP functional [27-31] and 6-31G(d,p) basis set [32-35] for all atoms except for ruthenium, for which LANL2DZ basis-set [36, 37] was applied. To compute electronic excitation spectra, Time Dependent – Density Functional Theory (TD-DFT) was used with the same functional and basis sets for light atoms, with LANL2DZ pseudo-potential for Ru. Eighty lowest laying electronic excitations were determined. All calculations were done with Gaussian 09 program [38], orbitals were visualized using GaussView [39] software.

2.4. Cell Culture Conditions

Biological studies were performed using murine colon carcinoma CT26 and human lung adenocarcinoma A549 cell lines. Cells were maintained in DMEM medium supplemented with 10% fetal bovine serum (FBS) and 1% antibiotics – penicillin (100 units/mL) and streptomycin (100 μg/mL). Cells were routinely cultured at 37 °C in a humidified incubator in a 5% CO_2 atmosphere.

2.5. Cytotoxicity

The evaluation of the cytotoxicity of the Ru complexes on A549 and CT26 cells, was conducted using an Alamar Blue assay. The Alamar Blue test is based on the reduction of blue and non-fluorescent subtrate (resazurin) to a pink and highly fluorescent product (resorufin) by the alive cells. Cells were seeded on a 96 wells plate with a density of 1.5×10^4 cells per cm^2 one day before the experiments. Then, cells were incubated with various concentrations of the Ru compounds and synthesized ligand L1 for 24/72 hours in the dark. All compounds were diluted in DMSO and then, added to the appropriate medium with or without 2% FBS to obtain the applied concentrations. The final DMSO concentration was kept constant at 0.1% (v/v) in case of **Ru2** and 0.5% (v/v) in case of **Ru1** and **bpySC**. After the incubation, cells were washed with PBS and incubated in the resazurin sodium salt solution (25 µM) for 3 h. The cell viability was quantified at 605 nm using 560 nm excitation light (Tecan Infinite 200 microplate reader). Experiments were performed in triplicate and repeated at least three times to get the mean values ± standard deviation. The viability was calculated with respect to the untreated cells control. The IC_{50} values were determined using the Hill equation (Origin 9.0) [40]

$$y = y_0 + \frac{(y_{100} - y_0)[c]^H}{[IC_{50}]^H + [c]^H}$$

2.6. Cellular imaging of accumulated Ru complexes

For co-localization experiments, A549 cells were seeded on a 6 well plate at a density of 3×10^4 cells per cm^2 24 h prior to the staining. ER-Trackert Blue-White DPX, Mitotracker Green and Lyso-Tracker Blue (Life Technologies) were used to image ER, mitochondria and lysosomes according to the manufacturer's protocols. The Ru complexes were incubated in basic medium for 24 h ([Ru1] = 500 µM, [Ru2] = 2 µM), then rinsed twice with PBS. The chosen concentration of the Ru complexes was not cytotoxic to the cells under these conditions. Images were acquired

using a Olympus fluorescence microscope IX51 equipped with an XC10 camera with 470–495 and 530–550 nm emission filters.

2.7. Cell cycle

A549 cells were seeded into a 6 wells plate with a density of 3×10^4 cells per cm^2. Cells were cultured in the full medium for 1 day. Then, the medium was removed and replaced with a basic medium containing various concentrations of the studied compounds, and incubated for 24 h. Then, the cells were washed with PBS, detached by trypsin, fixed in cold methanol for 30 min, stained with propidium iodide (PI) for 4 h in the dark, followed by analyzing using a BD LSRFortessa cytometer. The experiment was performed twice.

2.8. Apoptosis

The early stage of apoptosis is manifested by the relocation of phosphatidylserine (PS) from the inner side of the cellular membrane to the outer side. This process can be revealed by the staining cells with the labeled Annexin V. Annexin V is a cellular protein that in the presence of Ca^{2+} ions, selectively binds to PS. DAPI was used instead of propidium iodide to assess the cell necrosis, due to the overlapping excitation/emission parameter of the propidium iodide and the Ru complexes in live cells [41]. A549 cells were seeded into a 6 wells plate with a density of 3×10^4 cells per cm^2 and cultured in the full medium for 1 day. Afterwards, the medium was removed and replaced by a medium containing different amounts of the studied compounds and incubated for 24 h. Then, cells were washed with PBS and binding buffer. The cells were stained with Annexin V-FITC for 10 min in the dark and then, with DAPI (0.5 µM) for 5 min. Cells were analyzed by a BD LSRFortessa cytometer. As a positive control, H_2O_2 (300 µM) was used.

2.9. Caspases activity

Activation of caspases 3/7, 8 and 9 was examined using luminescent Caspase Glo assays (Promega) according to the manufacturer's manual. A549 and CT26 cells were seeded on a white 96 wells plate with a density of 1.6×10^4 cells per cm^2 24 h prior to the experiments. Next, the compounds at different concentrations were added to the wells and incubated for 24 h ([**Ru1**] = 200 µM, [**Ru2**] = 2 µM, [**bpySC**] = 100 µM). The luminescence intensity of the cells was measured using a Tecan Infinite 200 plate reader.

2.10. Mitochondrial morphology

MitoTracker Green (ThermoFisher Scientific) was used to visualize mitochondria of A549 cells. A549 cells were seeded on a 6 wells plate with a density of 3×10^4 cells per cm^2 24 h prior to the experiments. Next, the Ru complexes were added and incubated for 24 h. After the incubation, the Ru compounds were washed and cells were stained with MitoTracker Green (100 nM) for 30 min at 37 °C. After the staining, cells were visualized using an Olympus fluorescence microscope IX51.

2.11. Cytosolic calcium homeostasis

Cytosolic calcium concentration was measured using Fluo-8 AM probe (AAT Bioquest). A549 and CT26 cells were seeded on a 96 wells plate with a density of 1.5×10^4 cells per cm^2 one day before the experiments. Then, cells were incubated with various concentrations of the compounds for 24 h in the dark. Next, cells were washed with PBS and stained with Fluo-8 AM (4 µM) for 30 min in the dark at 37 °C. After staining cells were washed twice with PBS and analyzed by a Tecan Infinite 200 microplate reader measuring fluorescence of the probe at 525 nm using 490

nm as an excitation wavelength. Experiment was performed three times in triplicate and the mean values ± standard deviations were calculated.

2.12. Mitochondria membrane potential

Mitochondria membrane potential was evaluated using JC-1 probe (AAT Bioquest). A549 and CT26 cells were seeded on 96 wells plate with a density of 1.5×10^4 cells per cm^2 one day before the experiments. Cells were incubated with various concentrations of the Ru compounds for 24 h in the dark. Then, cells were washed with PBS and stained with JC-1 (10 µM) for 30 min in the dark at 37 °C. Next, cells were washed with PBS and analyzed by a Tecan Infinite 200 microplate reader measuring fluorescence of the probe at 525 nm and 590 nm using 490 nm as an excitation wavelength. Experiment was performed three times in triplicate and the mean values ± standard deviations were calculated.

2.13. Total ROS production

The level of the oxidative stress induced in cells after the incubation with the Ru complexes was conducted for A549 and CT26 cell lines using the cyto-ID Hypoxia/Oxidative stress detection kit. A549 and CT26 cells were seeded with a density of 3×10^4 cells per cm^2, respectively. A day later the compounds at different concentrations in medium without serum were added and incubated in the dark for 24/72 h. Then, cells were washed with PBS, treated with trypsin and analyzed by BD LSR cytometer. As a positive control, pyocyanin (300 µM) was used. The level of the oxidative stress was determined as a percentage of the ROS positive cells of the whole cell population.

3. Results and discussion

3.1 Synthesis

The preparation of the target complexes **Ru1** and **Ru2** required the synthesis of ligand **bpySC** (Scheme 2) that was synthesised by a Sonogashira coupling between 4-(but-3-yn-1-yl)-4'-methyl-2,2'-bipyridine (**3**) and 5-bromopyridine-2-carbaldehyde semicarbazone (**6**). **6** was synthesised by formylation of 5-bromo-2-iodopyridinefollowed by treatment with semicarbazide hydrochloride. **3** was synthesised by a selective monolithiation of 4,4'-dimethyl-2,2'-bipyridine (**1**) using LDA followed by reaction with 3-(trimethylsilyl)propagyl bromide and final deprotection using potassium bicarbonate [21].

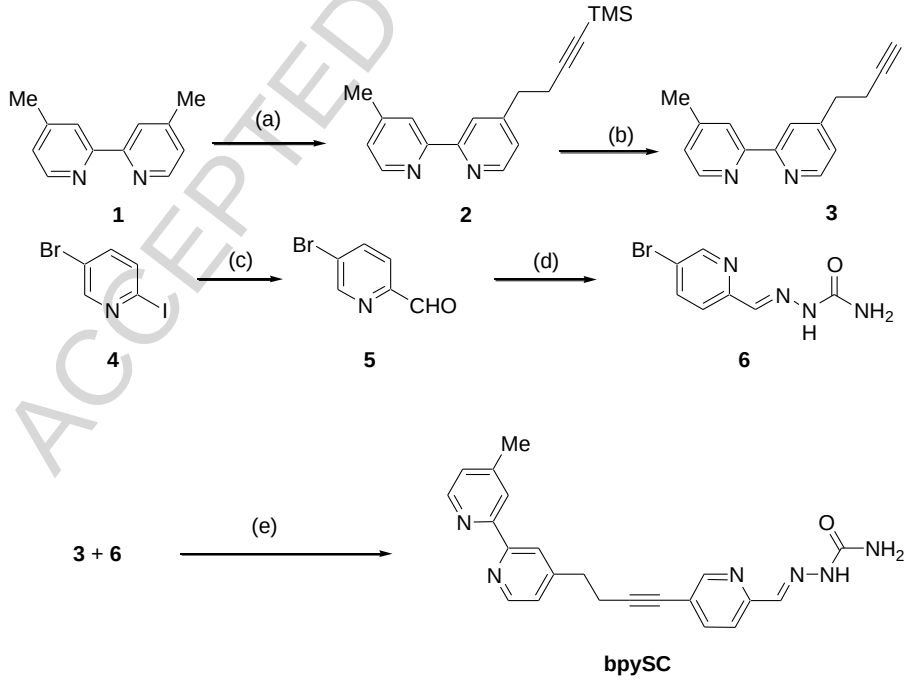

Scheme 2. Synthesis of ligand **bpySC** Reagents and conditions: (a) (1) LDA, -78ºC, THF, 0.5h then 0ºC, 2h; (3) 3-(trimethylsilyl)propagyl bromide, 1h; (b) K_2CO_3, MeOH, 50ºC, 2h; (c) (1) iPrMgCl, -10ºC, THF, 2h; (2) DMF, -10ºC -> RT 2h; (d) NH_2-NH-C(=O)-NH_2·HCl, EtOH, reflux, 3h; (e) CH_3CN, CuI, $Pd(PPh_3)_4$, diisopropylamine, reflux, 18h.

Complexes **Ru1** and **Ru2** were synthesised by refluxing *cis*-$Ru(NN)_2Cl_2$ complexes and **bpySC** in absolute ethanol. Dichlorobis(2,2'-bipyridine)ruthenium(II) ($Ru(bpy)_2Cl_2$) and dichlorobis(4,7-diphenyl-1,10-phenantroline)ruthenium(II) ($Ru(dip)_2Cl_2$) were used for **Ru1** and **Ru2,** respectively. The *cis*-$Ru(NN)_2Cl_2$ complexes were prepared by microwave synthesis from ruthenium(III) chloride and the proper ligand in DMF according to previously described procedures [42, 43]. Interestingly, the coordination of ruthenium occurred exclusively on the bipyridine side of the **bpySC** and no trace of ruthenium coordination by the SC moiety was observed.

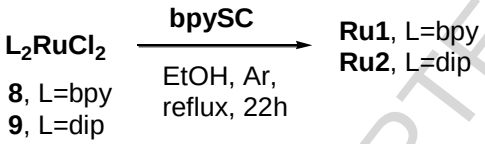

Scheme 3. Synthesis of **Ru1** and **Ru2**.

3.2. Photophysical properties

The complexes have been characterized by UV-Vis spectroscopy using water as solvent. The photophysical data are collected in Table 1. In order to measure the effect of **bpySC** on the properties, complexes containing one bpy instead of **bpySC** were prepared and characterized. As shown in Table 1 all complexes displayed intense ^{1}MLCT (metal ligand charge transfer) bands in the visible part of the spectrum, around 450 nm. Both **Ru1** and **Ru2** showed a slight red shift

compared with their unsubstituted counterparts. In contrast, the emission band exhibited a notable blue shift (11 nm for **Ru1** and 10 nm for **Ru2**). The introduction of the **bpySC** ligand also came with a decrease of the luminescence quantum yield (QY) that were 0.92% and 1.18% for **Ru1** and **Ru2** respectively under air-equilibrated conditions while argon-equilibrated conditions allowed to increase these values to 1.63%. and 2.62%, respectively. A decay of the MLCT excited state lifetimes was also observed for both **Ru1** and **Ru2.** Thus while globally affecting negatively the luminescence of the complexes, the **bpySC** ligand allowed to maintain QY and lifetimes exploitable for further use in imaging experiments**.**

Table 1. Photophysical properties of the ruthenium(II) complexes in air-equilibrated and deoxygenated aqueous solutions.

	Absorption		Emission (air-equilibrated conditions)			Emission (deoxygenated conditions)	
	λ_{max} [nm]	ε [M^{-1} cm^{-1}]	λ_{max} [nm]	Φ	τ [μs]	Φ	τ [μs]
$[Ru(bpy)_3]^{2+}$			628	0.0280[a]	0.37 ± 0.01	0.0420[b]	0.57 ± 0.01
	452	14 000					
$[Ru(dip)_2(bpy)]^{2+}$ [c]	279	88 100	613	0.0367 ± 0.0004	0.76 ± 0.01	0.1245 ± 0.0004	2.51 ± 0.01
	438	19 000					
	461	18 500					
Ru1	286	108 600	617	0.0092 ± 0.0009	0.27 ± 0.03	0.0162 ± 0.0002	0.36 ± 0.06
	427	15 400					
	455	18 100					
Ru2	279	204 800	623	0.0118 ± 0.0003	0.65 ± 0.03	0.0262 ± 0.0004	1.72 ± 0.07
	435	42 100					
	457	43 000					

data taken from [a] [24]; [b] [25]; [c] [44]

3.3. Computational characterization

Quantum chemical calculations within Density Functional Theory (DFT) approach allowed for determination of the **Ru1** and **Ru2** geometry structures (compare Supplementary Information) and characterization of their frontier orbitals (Fig. S1). In both complexes, HOMO spans over the **bpySC** ligand, whereas LUMO is delocalised over pyridine atoms of the remaining ligands of ruthenium: other bpys in **Ru1** and bpy fragment of **bpySC** in **Ru2**. Further, the performed Time-Dependent DFT (TD-DFT) calculations allowed for the characterisation of the spectra of both complexes. The most intensive bands clearly show the MLCT character of their visible – see Fig. 1 for schematic representation of their main features. In case of **Ru1**, the most intensive bands are centered around 421, 419 and 408 nm, and correspond to excitations from a mixture of Ru d and π bpy fragment of **bpySC** orbitals to π* orbitals of bpy ligands. In case of **Ru2**, they are present at around 441, 438, 427, 405, and 393 nm, and they might be attributed to the excitations from a mixture of Ru d and π orbitals of dip to π* orbitals of the bpy fragment of **bpySC**.

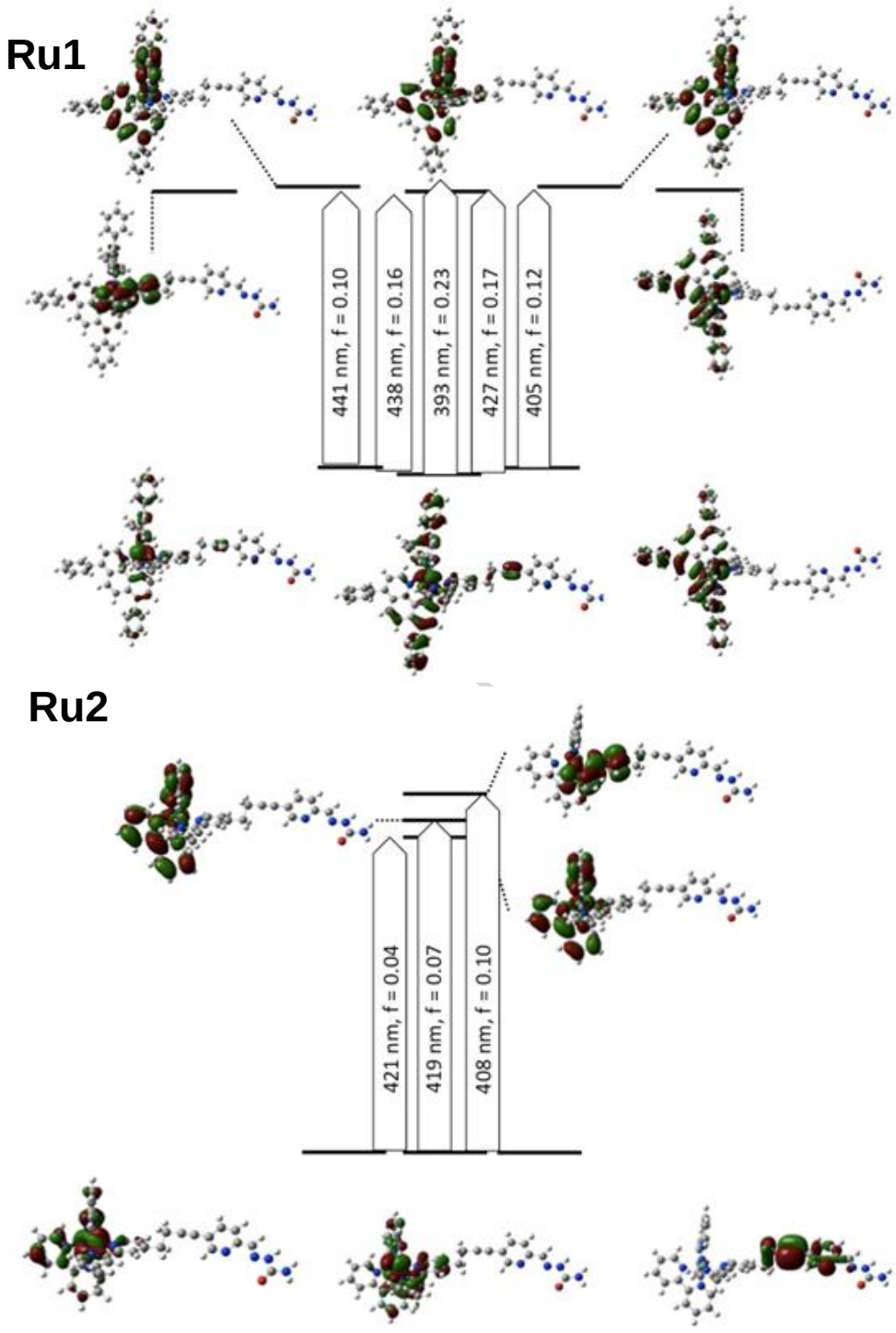

Fig. 1. Plots of orbitals responsible for the most intensive absorption bands in the visible range of **Ru1** and **Ru2** spectra with schematic representation of the most intense absorption bands, as computed with TD-DFT.

3.4. Cytotoxicity of ruthenium complexes *in vitro*

The cytotoxic effect of the newly synthesised Ru complexes and their reference compounds was determined on two cancer cell lines: murine colon carcinoma (CT26) and human lung adenocarcinoma cell line (A549). Complexes were tested in serum free conditions (S-) and also in the presence of 2% serum (S+). The obtained results are presented in Table 2. Generally, the presence of serum reduced the cytotoxic effect of both **Ru1** and **Ru2**. Such an effect has been previously described [45] and might be related to a reduction in the Ru uptake due to binding to the proteins present in the serum (see Table S1) impeding complexes accumulation. Ru complexes with dip ligands were much more cytotoxic in comparison with those having bpy ones. Replacing one of the dip ligands with bpy or **bpySC** ligand decreases slightly the cytotoxicity of the Ru compounds. The observed effect arises from the dependence of the Ru complexes accumulation and therefore their toxicity on their lipophilicity. In agreement with some previous studies on Ru polypyridyl complexes [44], the poor cellular uptake of $[Ru(bpy)_3]^{2+}$ or **Ru1** can be related to their weak lipophilic character.

Increasing the incubation time from 24 to 72 h resulted in a distinct increase in an anti-proliferative activity of **Ru1**, in particular against CT26 cells, while no significant change was observed in the cytotoxicity of **Ru2**. $[Ru(bpy)_3]^{2+}$ remains continuously non cytotoxic even after 72 h of incubation. At the same time a dramatic increase in the toxicity after 72 h was observed for **bpySC** ligand alone (IC_{50} ca. 30 times higher). It suggests that this particular ligand might play a crucial role in the anti-proliferative activity of **Ru1**. Furthermore, it can be assumed that an appropriate selection of auxiliary ligands might lead to a change in action mechanism. For the studied system, switching from two dip ligands to two bpy ones clearly highlighted the cytotoxic

activity of **bpySC** ligand in **Ru1**, whereas in **Ru2** compound these two auxiliary dip ligands played a key role.

Table 2. IC_{50} of Ru complexes against two cancer cell lines A549 and CT26. Experiments were performed in medium without (S-) or with (S+, 2%) serum.

		IC_{50} (µM) 24h		**IC_{50} (µM) 72 h**	
		S-	S+	S-	S+
A549	**bpySC**	102 ± 59	-	2.8 ± 0.8	3.3 ± 1.2
	Ru1	113 ± 154	202 ± 17	97 ± 14	138 ± 20
	Ru2	6.8 ± 1.2	9.8 ± 2.3	9.0 ± 1.9	16 ± 2
	$[Ru(dip)_2(bpy)]^{2+}$	4.0 ± 0.7	-	-	-
	$[Ru(bpy)_3]^{2+}$	>320	>320	>320	>320
	$[Ru(dip)_3]^{2+}$	1.2 ± 0.1	-	-	-
CT26	**bpySC**	96 ± 28	-	1.5 ± 0.3	2.0 ± 0.3
	Ru1	201 ± 25	233 ± 38	31 ± 11	50 ± 7.6
	Ru2	4.6 ± 0.9	5.0 ± 0.1	5.7 ± 1.5	21 ± 5
	$[Ru(dip)_2(bpy)]^{2+}$	3.4 ± 0.7	-	-	-
	$[Ru(bpy)_3]^{2+}$	>320	>320	>320	>320
	$[Ru(dip)_3]^{2+}$	1.2 ± 0.2	-	-	-

3.5. Cell accumulation and cellular targets

A549 cells were used to study the accumulation of the studied ruthenium complexes. A higher cellular uptake was found for complex **Ru2** in excellent agreement with the cytotoxicity data.

Despite similar luminescence quantum yields for **Ru2** and **Ru1**, much higher concentrations of **Ru1** were required to visualize its localization inside the cells. This further confirmed that the accumulation of ruthenium polypyridyl complexes is strongly dependent on their lipophilicity and that in the studied case it is controlled by bpy/dip ligands. Additionally, it points out the superiority of the accumulation/lipophilicity parameters over luminescence parameters of Ru complexes in assessing the potential of the compounds as cellular dyes [44].

To further investigate the accumulation of the Ru complexes, organelle-specific dyes were used. **Ru2** preferably accumulated into mitochondria and endoplasmic reticulum, as confirmed by overlapping emission of organelle-specific dyes with the studied Ru complex (Fig. 2). Complex **Ru1** exhibited rather small accumulation in those organelles (Fig. S2), while the majority of it is localized within cellular lysosomes (Fig. 3).

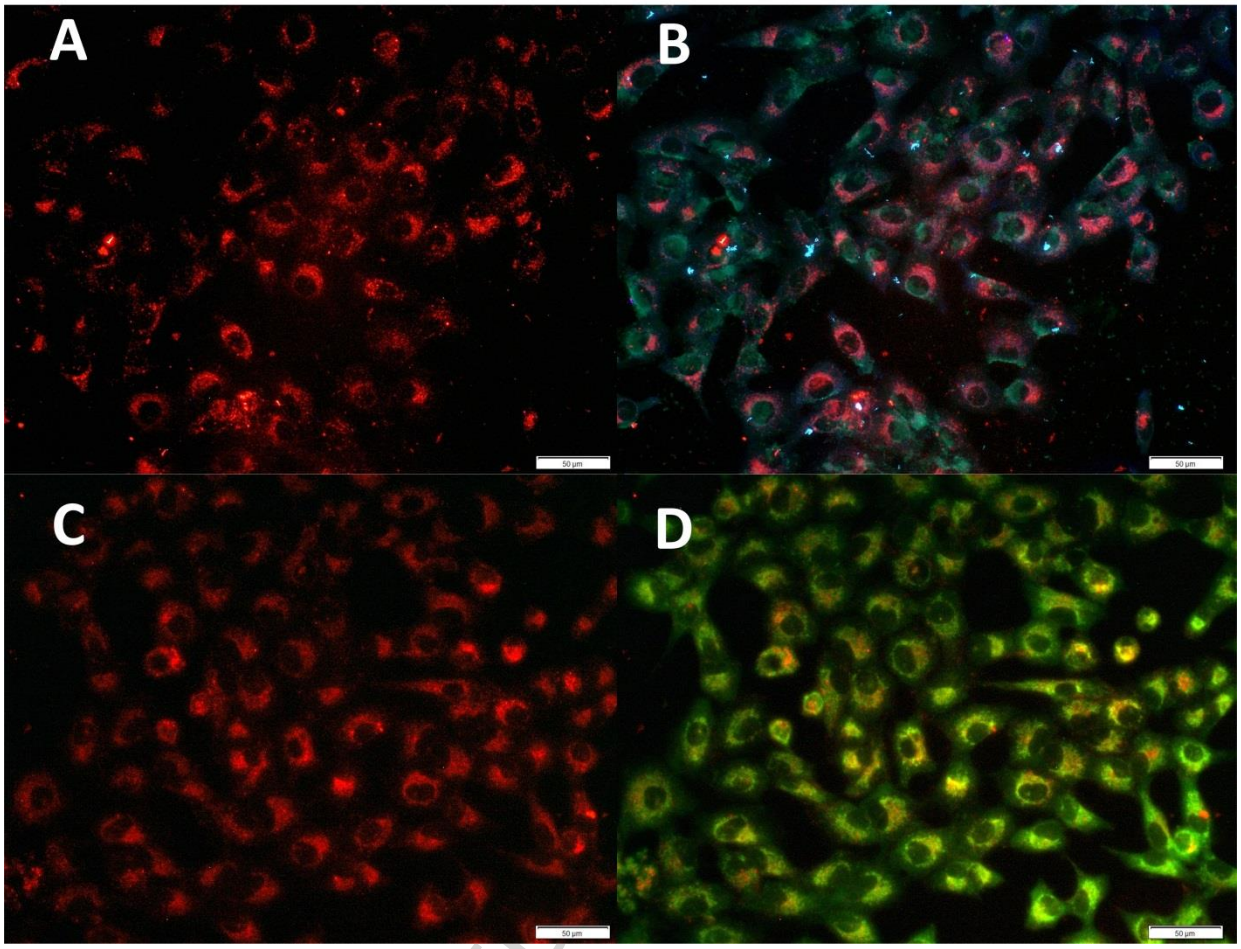

Fig. 2. Fluorescence images of A549 cells showing subcellular localization of **Ru2** (2 μM, incubation 24 h). (A,C) red colour comes from **Ru2** complex emission; (B) ER-Tracker Blue was used to image endoplasmic reticulum, blue colour arises from organelle-specific dye while pink colour represents overlap of the red luminescence of Ru and blue emission from dye indicating co-localization; (D) MitoTracker Green was used to image mitochondria and green colour arises from organelle-specific dye, while yellow colour represents overlap of the red luminescence of Ru and green emission from dye indicating co-localization. Scale bars 50 μm.

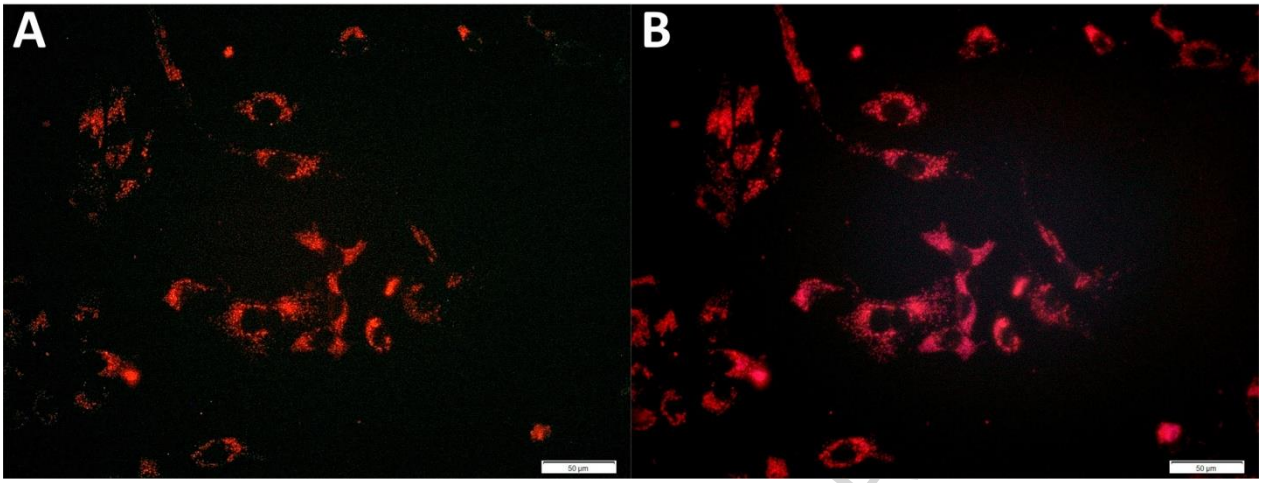

Fig. 3. Fluorescence images of A549 cells showing subcellular localization of **Ru1** (500 μM, incubation 24 h). (A) Red colour comes from **Ru1** complex emission; (B) LysoTracker Blue was used to image lysosomes, pink colour represents overlap of the red luminescence of Ru and blue emission from dye indicating co-localization. Scale bars 50 μm.

3.6. Cell-cycle arresting properties

The influence of **Ru1**, **Ru2** and **bpySC** on cell cycle was measured by flow-cytometry (Table 3). The incubation of A549 cells with **Ru1** or **bpySC** induced a significant increase in the number of cells in the S-phase of the cell cycle, with the corresponding decrease in the percentage of cells in the G2/M phase. During the S-phase of the cell cycle deoxyribonucleotides, which are DNA precursors, are produced. In this phase, corresponding ribonucleotides need to be reduced by ribonucleotide reductase. Inhibition of this enzyme should increase the number of cells arrested in this phase [46, 47]. The S-phase arrest caused by **Ru1** or **bpySC** suggests that their cellular activities might be related to the inhibition of ribonucleotide reductase. Contrarily **Ru2** caused increased percentage of the cells in the G0/G1 phase, similarly to other Ru complexes containing

dip ligands [45]. This further confirms the influence of the auxiliary ligands on the biological activity of Ru compounds.

Table 3. Cell cycle distribution of A549 cells after 24 h treatment with the Ru polypyridyl complexes and with ligand **bpySC** (representative analysis).

	G0/G1	S-phase	G2/M
Control	57.5%	36.0%	6.5%
bpySC	22.2%	74.0%	3.8%
Ru1	47.5%	48.4%	4.1%
Ru2	76.9%	22.5%	0.6%

3.7. Reactive Oxygen Species (ROS) production

The influence of **Ru1** and **Ru2** on reactive oxygen species (ROS) production in cancer cell lines was evaluated. **Ru2** as well as the attached ligand **bpySC** caused significant concentration dependent increase in ROS production after 24 of h incubation in both A549 and CT26 cell lines (Fig. 4, Fig. S3). Increasing the incubation time 24 h to 72 h also increase the ROS level induced by **Ru2**. However, **Ru1** did not induce oxidative stress in the studied cell lines that could be partially explained by the lower accumulation of this complex. However increasing the incubation time with the compounds from 24 h to 72 h (that will also increase Ru complexes accumulation level) did not induce any increase in ROS production in case of **Ru1** as it did with **Ru2** (Fig. 4). This strongly suggested that the Ru accumulation level is not linked to the lack of ROS production in case of **Ru1** and that completely different action mechanism of action responsible for cytotoxic activity depending on whether bpy or dip ligand is present in the ruthenium complex.

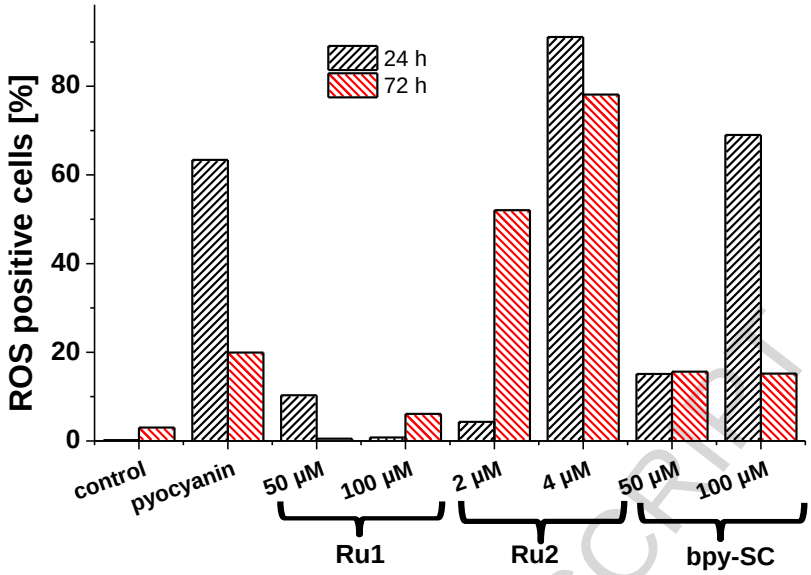

Fig. 4. The level of oxidative stress induced in A549 cells after 24 and 72 h treatment with the Ru polypyridyl complexes expressed as percentage of ROS positive cells in the whole cell population (%). Pyocyanin was used as ROS positive control.

3.8. Apoptosis inducing properties

The determination of the cellular death mechanism was performed using flow cytometry. A549 cells were double stained with Annexin-V- FITC conjugate and DAPI after incubation with **Ru1**, **Ru2** and **bpySC** for 24h. Incubation with all studied compounds significantly increased the population of Annexin V-positive cells, indicating cells undergoing early phase of apoptosis (Fig. 5), with no indication of the DAPI-positive cells that would suggest a necrotic cellular death. Despite lesser accumulation of **Ru1**, that was previously confirmed by the cytotoxicity and localization study, this compound was found to be powerful apoptosis inducing agent.

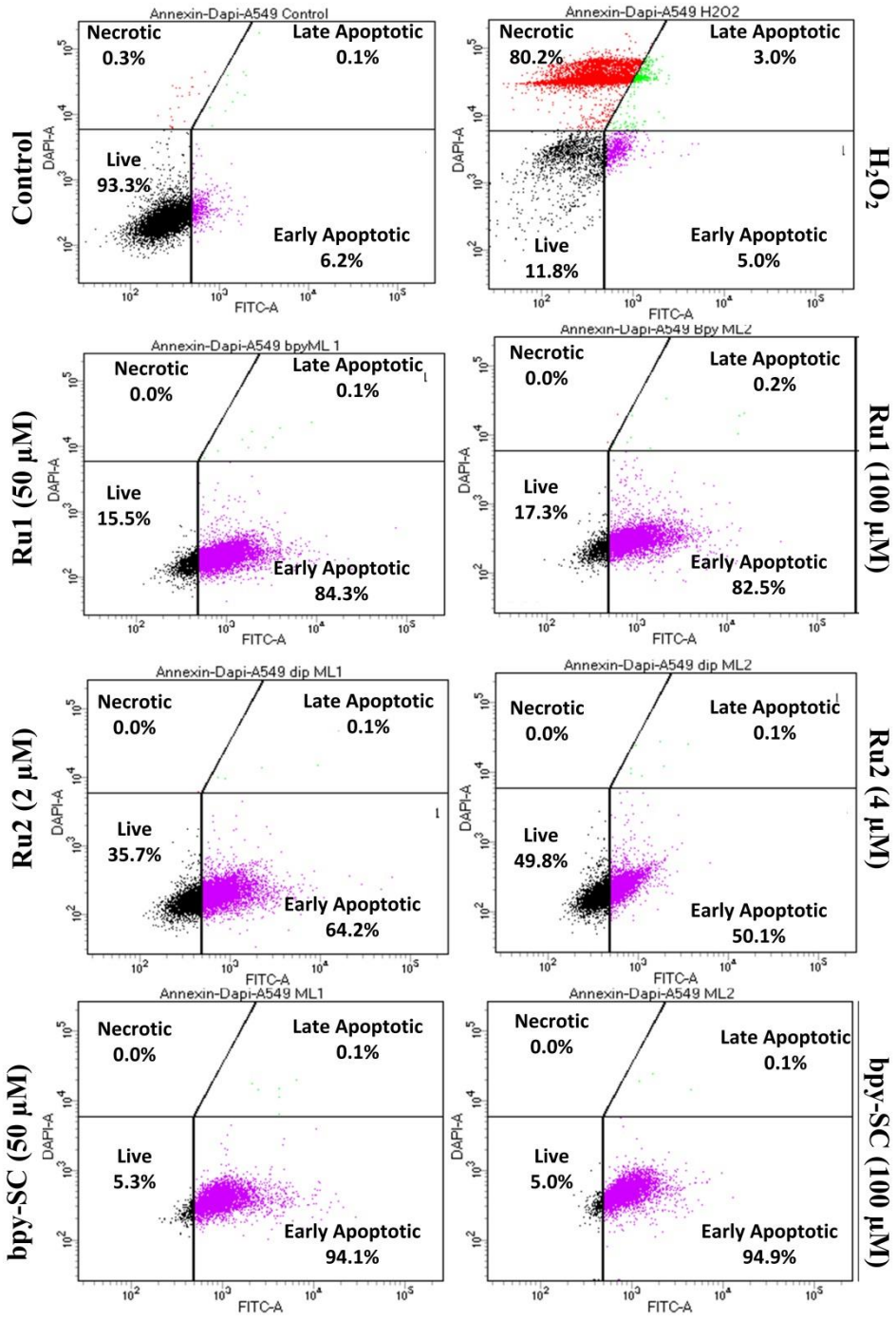

Fig. 5. Apoptosis of A549 cells upon 24 h exposure to the Ru polypyridyl complexes. Cells were labeled with Annexin V-FITC/DAPI.

3.9. Activation of the signalling pathways - caspases activity

Early morphological signs of apoptosis such as translocation of phosphatidylserine are a result of a cascade of biochemical changes occurring within the cell. To further explore the developed changes and investigate the apoptotic mechanism of cellular death of cancer cell lines, caspases activity was measured (Fig. 6). After incubation of A549 and CT26 cells with **Ru2**, no caspase activation was observed, indicating that the observed apoptosis occurred via caspase-independent pathway. On the contrary, incubation of cells with **Ru1** and **bpySC** induced significant increase in activity of initiator caspase 9 and effector caspases 3/7, while no activation of caspase 8 was detected. This indicates that **Ru1** and **bpySC** triggered apoptotic cellular death via intrinsic mitochondrial pathway.

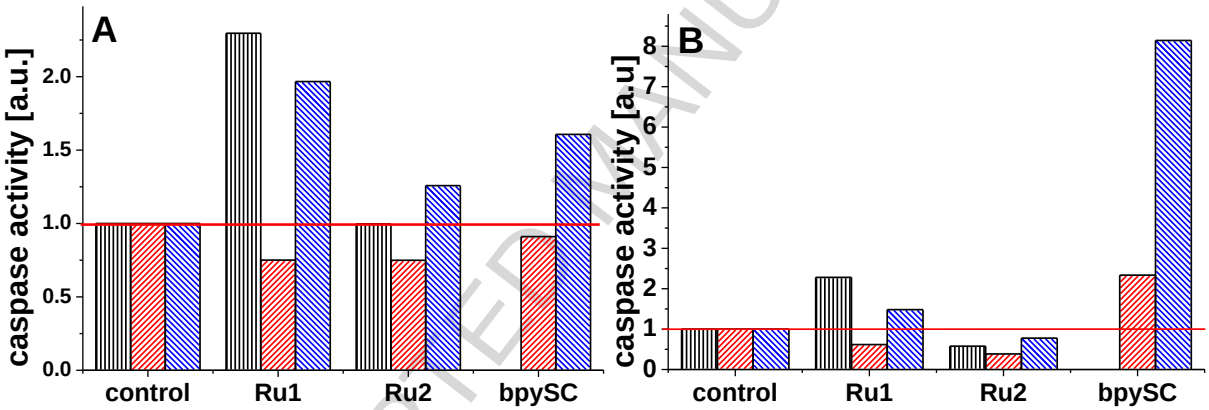

Fig. 6. Caspases 3/7 (black), 8 (red) and 9 (blue) activities after 24 h exposure to the Ru polypyridyl complexes and ligand **bpySC** determined in A549 (A) and CT26 (B) cell lines.

This conclusion is further supported by the visualization of the mitochondria of the Ru treated cells (Fig. 7). While no significant change is observed in mitochondria of **Ru2** treated cell, incubation of cells with **Ru1** caused swelling and enlarging of mitochondria. Such process is often observed in case of apoptotic cell death induced by mitochondria pathway.

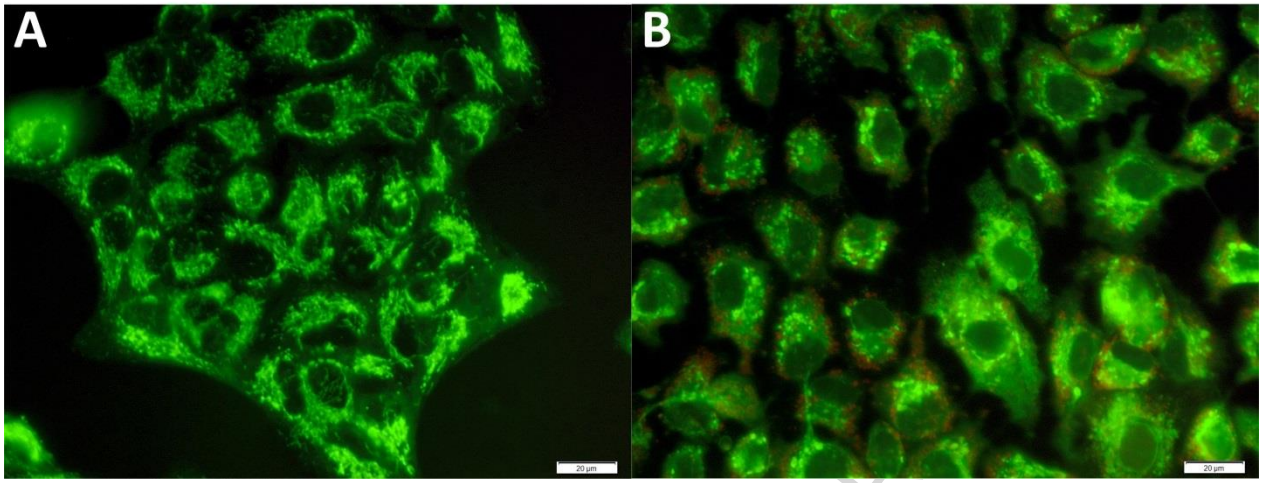

Fig. 7. Fluorescence images of A549 cells showing swelling and enlarging of mitochondria after treatment with **Ru1**. MitoTracker Green was used to image mitochondria and green colour arises from a organelle-specific dye (A) untreated cells; (B) cells treated with **Ru1** (500 μM) for 24 h. Scale bars 50 μm.

3.10. Mitochondrial membrane potential detection

Since the studied Ru complexes either accumulated in mitochondria (**Ru2**) or changed the mitochondria morphology (**Ru1**), their influence on alteration in mitochondria function was also studied by analyzing the mitochondria membrane potential. The loss of the mitochondria membrane potential is often considered to be a prelude to apoptosis.

The changes of mitochondrial membrane potential induced by the studied complexes were determined using JC-1 mitochondrial probe. At low mitochondrial membrane potential, JC-1 exists in monomeric form and exhibits green fluorescence, but at high mitochondrial membrane potential JC-1 forms aggregates, which exhibit red fluorescence. Two oligopeptides valinomycin and gramicidin were used as positive controls. Valinomycin is K^+ ionophore which allows the potassium ions passing freely through the cell membrane and in this way causing the collapse of

mitochondrial membrane potential. Gramicidin is another polypeptide which forms channels in phospholipid membranes and allows ions to pass freely through the membrane leading to the decrease in $\Delta\Psi_m$. The change of mitochondrial potential was represented as change of red/green fluorescence ratio and the results are shown in Fig. 8. All tested compounds caused the decrease in red/green fluorescence intensity ration, indicating depolarization of mitochondria membrane. The effect is stronger in CT26 cells. These results further confirm that **Ru1** and **bpySC** induces apoptosis in cancer cells through the mitochondrial signal transduction pathway.

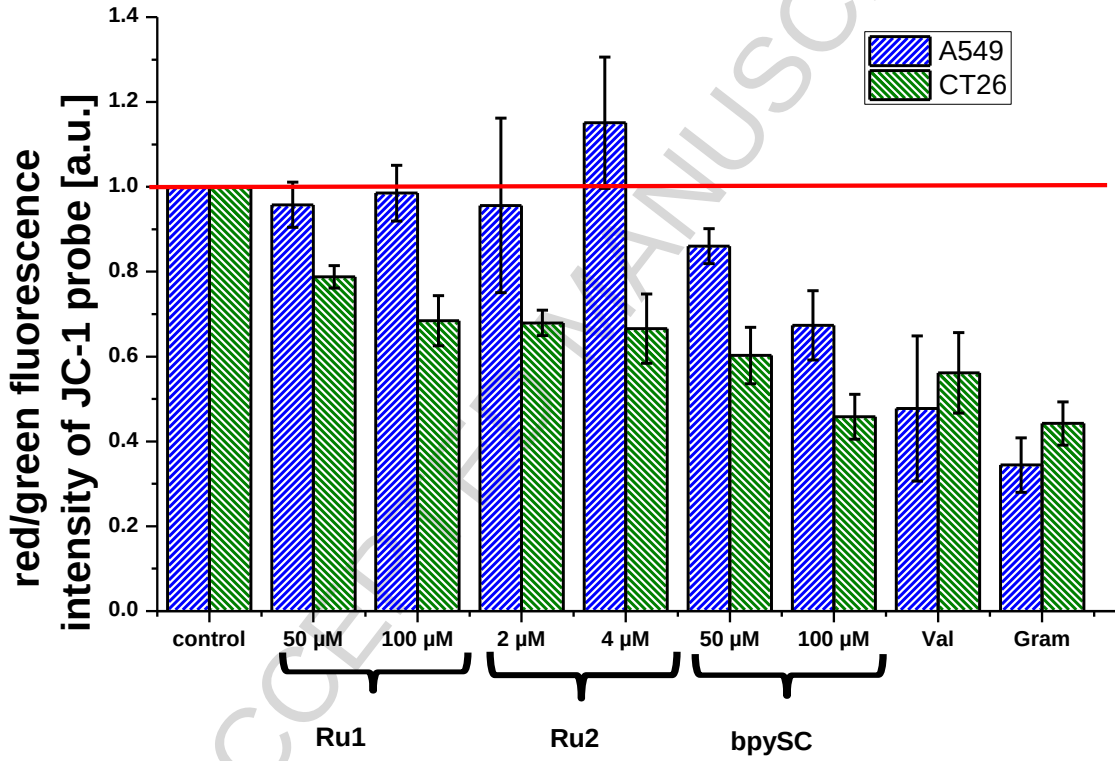

Fig. 8. Effect of the Ru polypyridyl complexes on mitochondrial membrane potential ($\Delta\Psi_m$) in A549 and CT26 cell lines after 24 h treatment measured using JC-1 probe. The results are representative at least three independent experiments. Red fluorescence corresponds to the fluorescence of J-aggregates, while green fluorescence is related to the fluorescence of J-monomers. The decrease in a ratio of red to green fluorescence values indicates depolarization of

mitochondria membrane potential. Valinomycin (Val) and gramicidin (Gram) were used as positive controls.

3.11. Intracellular calcium concentration

Calcium ion is one of the most important signal transducers in cells, involved in numerous physiological and pathological processes. It is known that a variety of metals complexes are able to modify intracellular Ca^{2+} signalling and hence induce apoptosis or necrosis [48, 49]. Using Fluo-8 AM probe the changes in intracellular calcium concentration ($[Ca^{2+}]_C$) in cancer cells after 24 h incubation with the studied compounds were monitored. The results are presented in Fig. 9. Alteration in calcium homeostasis upon treatment with the Ru complexes was cell line dependent. In case of A549 cells, no significant changes in $[Ca^{2+}]_C$ after treatment with **Ru1** or **bpy-SC** were observed. Only **Ru2** accumulation caused a decrease in cytosolic calcium level, and this effect had been already observed previously with other polypyridyl Ru complexes containing dip ligands [50].

Accumulation of **Ru1** in CT26 cell line resulted in concentration dependent decrease in intracellular calcium level, while **Ru2** and **bpySC** caused the opposite effect - increasing the calcium ions concentration. Such an increase in $[Ca^{2+}]_C$ can cause a rise in mitochondrial calcium levels since those organelles serves as buffering units and might modulate Ca^{2+} feedback-inhibition or activation mechanisms. Increase in the mitochondrial calcium concentration can cause the mitochondrial membrane depolarization and lead to higher amounts of reactive oxygen species production. This can force the opening of the mitochondrial permeability pore causing mitochondrial swelling and releasing cytochrome c and other pro-apoptotic factors, initiating programmed cell death process.

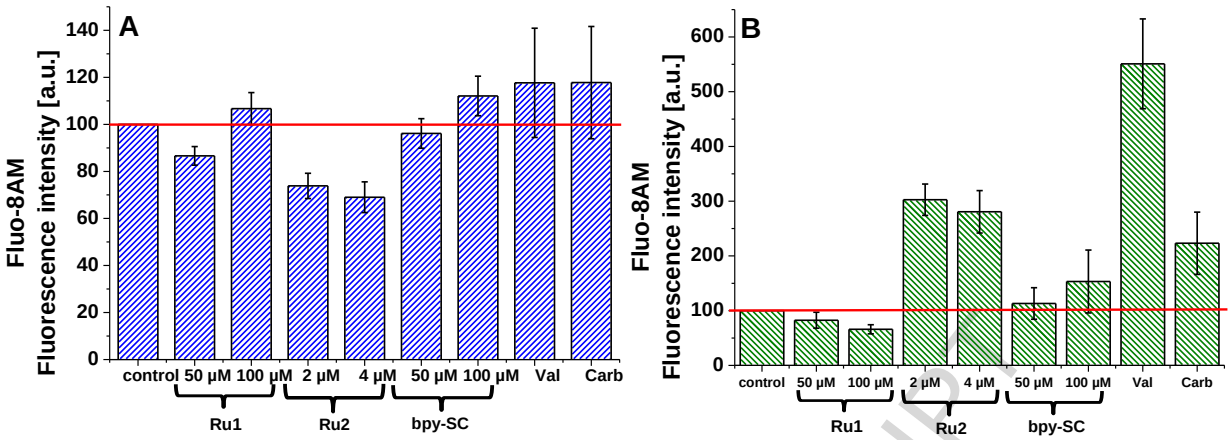

Fig. 9. The effect of the Ru polypyridyl complexes on cytosolic calcium cations concentration measured with Fluo-8AM in A549 (A) and CT26 (B) cell lines after 24 of incubation. The results are representative for three independent experiments performed in triplicate. Valinomycin (Val) and carbachol (Carb) were used as positive controls.

4. Conclusions

A new ligand based on semicarbazone 2-formylopyridine moiety conjugated with 2,2'-bipyridyl (**bpySC**) by an alkyne spacer has been developed. The two compounds produced as a result of coordination by ruthenium(II) center by **bpySC** and either two bpy (**Ru1**) or two dip (**Ru2**) ligands have been obtained and characterized. They exhibited entirely different biological effects on cancer cell lines. The cytotoxic effect determined after 24 h of treatment with **Ru2** was more than an order of magnitude higher than that found for **Ru1** as well as **bpySC** ligand alone against both A549 and CT26 cancer cell lines. The extent of treatment up to 72 h resulted in the increased anti-proliferative activity of both **Ru1** and **bpySC** but not of **Ru2**. The **Ru1** complex accumulated preferentially in lysozyme, while **Ru2** in mitochondria and endoplasmic reticulum. Both Ru complexes and **bpySC** induced apoptosis. In the case of **Ru2** it occurred via caspase-independent pathway, while **Ru1** and **bpySC** induced apoptosis in cancer cells through

mitochondria signal transduction pathway, even though this organelle was not the primary localization site. Both studied ruthenium complexes had an opposite effect on intracellular calcium concentration. The increased in ROS production was evident upon treatment with **Ru2** while negligible for **Ru1** even after prolonged incubation time.

Taken together we have demonstrated that changing of bpy into dip ligands has a strong impact on the mechanism of biological activity of the ruthenium(II) complexes. Despite increasing the Ru complexes overall accumulation and cytotoxicity by choosing the more lipophilic dip ligands the role of the semicarbazone 2-formylopyridine moiety in biological activity of the ruthenium complex seems to be marginal. Therefore, a special attention must be paid in choosing appropriate auxiliary ligands in designing new ruthenium complexes to take advantage from conjugation of biologically active molecules to polypyridyl ligands.

Abbreviations

A549 – and human lung adenocarcinoma cell line;

bpy – 2,2'-bipyridine;

bpySC – 5-(4-{4'-methyl-[2,2'-bipyridine]-4-yl}but-1-yn-1-yl)pyridine-2-carbaldehyde semicarbazone;

CT26 – murine colon carcinoma cell line;

DAPI – 4',6-diamidino-2-phenylindole;

DFT – Density Functional Theory;

dip – 4,7-diphenyl-1,10-phenanthroline;

DMEM – Dulbecco's Modified Eagle's medium;

DMF – dimethylformamide;

EtOH – ethanol;

ER – endoplasmic reticulum;

ESI – electrospray ionization;

FBS – fetal bovine serum;

FITC – fluorescein isothiocyanate;

HOMO – highest occupied molecular orbital;

HRMS – high resolution mass spectrometry;

IC_{50} – concentration causing 50 % decrease in viability;

iPrMgCl – Isopropylmagnesium chloride;

JC-1 – 5,5,6,6-Tetrachloro-1,1,3,3-tetraethylbenzimidazolylcarbocyanine iodide;

LDA – lithium diisopropylamide;

LUMO – lowest unoccupied molecular orbital;

MeOH – methanol;

MLCT – metal ligand charge transfer;

NMR – nuclear magnetic resonance;

QY – quantum yield;

PBS – phosphate buffered saline;

PI – propidium iodide;

ROS – reactive oxygen species;

RR – ribonucleotide reductase;

S- – in serum free conditions;

S+ – in the presence of 2%;

THF – tetrahydrofuran;

TD-DFT – Time-Dependent DFT.

Acknowledgements

The CNRS and French Ministry of Research are thanked for their support. M. Ł. acknowledges the French Embassy in Poland for providing a cotutelle Ph.D. grant. O. M. acknowledges the financial support from the National Science Center (DEC-2013/11/N/ST5/01606). M. B. acknowledges the financial support from the National Science Center (DEC-2016/21/B/NZ7/01081). This work was carried out using the equipment purchased through financial support from the European Regional Development Fund in the framework of the Polish Innovation Economy Operational Program (contract no. POIG.02.01.00-12-023/08). This research was supported in part by PL-Grid Infrastructure.

References

[1] A. Bergamo, G. Sava, Dalton Trans. 40 (2011) 7817-7823.

[2] C. Avendano, J.C. Menendez, Medicinal chemistry of anticancer drugs, Elsevier, 2008.

[3] L.N. Lameijer, S.L. Hopkins, T.G. Breve, S.H.C. Askes, S. Bonnet, Chem. Eur. J 22 (2016) 18484-18491.

[4] L. Blackmore, R. Moriarty, C. Dolan, K. Adamson, R.J. Forster, M. Devocelle, T.E. Keyes, Chem. Commun. 49 (2013) 2658-2660.

[5] K.K.W. Lo, T.K.M. Lee, J.S.Y. Lau, W.L. Poon, S.H. Cheng, Inorg. Chem. 47 (2008) 200-208.

[6] R.R. Ye, Z.F. Ke, C.P. Tan, L. He, L.N. Ji, Z.W. Mao, Chem.-Eur. J. 19 (2013) 10160-10169.

[7] O. Mazuryk, M. Maciuszek, G. Stochel, F. Suzenet, M. Brindell, J. Inorg. Biochem. 134 (2014) 83-91.

[8] A. Son, A. Kawasaki, D. Hara, T. Ito, K. Tanabe, Chem. Eur. J 21 (2015) 2527-2525-2536.

[9] G. Shi, S. Monro, R. Hennigar, J. Colpitts, J. Fong, K. Kasimova, H.M. Yin, R. DeCoste, C. Spencer, L. Chamberlain, A. Mandel, L. Lilge, S.A. McFarland, Coord. Chem. Rev. 282 (2015) 127-138.

[10] J.X. Zhang, J.W. Zhou, C.F. Chan, D.W.J. Kwong, H.L. Tam, N.K. Mak, K.L. Wong, W.K. Wong, BioConjugate Chem. 23 (2012) 1623-1638.

[11] J. Yang, Q. Cao, W.-L. Hu, R.-R. Ye, L. He, L.-N. Ji, P.Z. Qinb, Z.-W. Mao, Dalton Trans. 46 (2017) 445-454.

[12] S.M.H. Ali, Y.-K. Yan, P.P.F. Lee, K.Z.X. Khong, M.A. Sk, K.H. Lim, B. Klejevskajac, R. Vilarc, Dalton Trans. 43 (2014) 1449-1459.

[13] T.K. Venkatachalam, P.V. Bernhardt, C.J. Noble, N. Fletcher, G.K. Pierens, K.J. Thurecht, D.C. Reutens, J. Inorg. Biochem. 162 (2016) 295-308.

[14] J.T. Wilson, X.H. Jiang, B.C. McGill, E.C. Lisic, J.E. Deweese, Chem. Res. Toxicol. 29 (2016) 649-658.

[15] J. O'Neill, (2016).

[16] C.A. Kunos, T. Radivoyevitch, S. Waggoner, R. Debernardo, K. Zanotti, K. Resnick, N. Fusco, R. Adams, R. Redline, P. Faulhaber, A. Dowlati, Gynecol. Oncol. 130 (2013) 75-80.

[17] N.S.H.N. Moorthy, N.M.F.S.A. Cerqueira, M.J. Ramos, P.A. Fernandes, Mini-Rev. Med. Chem. 13 (2013) 1862-1872.

[18] A.I. Matesanz, P. Souza, Mini-Rev. Med. Chem. 9 (2009) 1389-1396.

[19] W.L.E. Armarego, C.L.L. Chai, , , Purification of Laboratory Chemicals, 5th ed., Elsevier, 2003.

[20] M.C. Pirrung, The Synthetic Organic Chemist's Companion, Wiley, New Jersey, 2007.

[21] J.J. Song, N.K. Yee, Z. Tan, J. Xu, S.R. Kapadia, C.H. Senanayake, Org. Lett. (2004) 4905-4907.

[22] T. Togano, N. Nagao, M. Tsuchida, H. Kumakura, K. Hisamatsu, F. Howell, M. Mukaida, Inorg. Chim. Acta 195 (1992) 221-225.

[23] R. Caspar, C. Cordier, J.B. Waern, C. Guyard-Duhayon, M. Gruselle, P. Le Floch, H. Amouri, Inorg. Chem. 45 (2006) 4071-4078.

[24] J.B. Waern, C. Desmarets, L. Chamoreau, H. Amouri, A. Barbieri, C. Sabatini, B. Ventura, F. Barigelletti, Inorg. Chem. 47 (2008) 3340-3348.

[25] R.B. Nair, B.M. Cullum, C.J. Murphy, Inorg. Chem. 36 (1997) 962-965.

[26] J.R. Lakowicz, Principles of Fluorescence Spectroscopy, Third Edition ed., Springer, 2006.

[27] P.A.M. Dirac, Proceedings of the Royal Society of London. Series A 123 (1929) 714-733.

[28] J.C. Slater, Physical Review 81 (1951) 385-390.

[29] S.H. Vosko, L. Wilk, M. Nusair, Canadian Journal of Physics 58 (1980) 1200-1211.

[30] A.D. Becke, Physical Review A 38 (1988) 3098-3100.

[31] C. Lee, W. Yang, R.G. Parr, Physical Review B 37 (1988) 785-789.

[32] R. Ditchfield, W.J. Hehre, J.A. Pople, J. Chem. Phys. 54 (1971) 724-728.

[33] W.J. Hehre, R. Ditchfield, J.A. Pople, J. Chem. Phys. 56 (1972) 2257.

[34] P.C. Hariharan, J.A. Pople, Theor. Chem. Acc. 28 (1973) 213-222.

[35] M.M. Francl, W.J. Pietro, W.J. Hehre, J.S. Binkley, D.J. DeFrees, J.A. Pople, M.S. Gordon, J. Chem. Phys. 77 (1982) 3654-3665.

[36] P.J. Hay, W.R. Wadt, J. Chem. Phys. 82 (1985) 270-283.

[37] W.R. Wadt, P.J. Hay, J. Chem. Phys. 82 (1985) 284.

[38] M. J. Frisch, G.W. Truck, H. B. Schlegel, G. E. Scuseria, M. A. Robb, J. R. Cheeseman, G. Scalmani, V. Barone, G. A. Petersson, H. Nakatsuji, M.C. X. Li, A. Marenich, J. Bloino, B. G. Janesko, R. Gomperts, B. Mennucci, H. P. Hratchian, J. V. Ortiz, A. F. Izmaylow, J. L. Sonnenberg, D. Williams-Young, F.L. F. Ding, F. Egidi, J. Goings, B. Peng, A. Petrone, T.

Henderson, D. Ranasinghe, V. G. Zakrzewski, J. Gao, N. Rega, G. Zheng, W. Liang, M. Hada, M. Ehara, K. Toyota, R. Fukuda, J. Hasegawa, M. Ishida, T. Nakajima, Y. Honda, O. Kitao, H. Nakai, T. Vreven, K. Throssell, J. A. Montgomery, J.E.P. Jr., F. Ogliaro, M. Bearpark, J. J. Heyd, E. Brothers, K. N. Kudin, V. N. Staroverov, T. Keith, R. Kobayashi, J. Normand, K. Raghavachari, A. Rendell, J. C. Burant, S. S. Iyengar, J. Tomasi, M. Cossi, J. M. Millam, M. Klene, C. Adamo, R. Cammi, J. W. Ochterski, R. L. Martin, K. Morokuma, O. Farkas, J. B. Foresman, D. J. Fox, , 2016., Gaussian, Inc., in, vol. Gaussian 09, Wallingford CT, 2016

[39] R. Dennington, T.A. Keith, J.M. Millam, GaussView, Version 6, , in, Semichem Inc., Shawnee Mission, KS, 2016.

[40] J. Weyermann, D. Lochmann, Z. A., Int. J. Pharm. 288 (2005) 369-376.

[41] A. Lorents, P.K. Kodavali, N. Oskolkov, U. Langel, M. Hällbrink, M. Pooga, J. Biol. Chem. 287 (2012) 16880–16889.

[42] D. Martineau, M. Beley, P.C. Gros, S. Cazzanti, S. Caramori, C.A. Bignozzi, Inorg. Chem. 46 (2007) 2272-2277.

[43] O.V. Kharissova, B.I. Kharisov, U.O. Méndez, Microwave-assisted synthesis of coordination and organometallic compounds, in: G. Grundas (Ed.) Advances in induction and microwave heating of mineral and organic materials, InTech, 2011.

[44] O. Mazuryk, K. Magiera, B. Rys, F. Suzenet, C. Kieda, M. Brindell, J. Biol. Inorg. Chem. 19 (2014) 1305-1316.

[45] O. Mazuryk, F. Suzenet, C. Kieda, M. Brindell, Metallomics 7 (2015) 553-566.

[46] N. Sanvisens, R. de Llanos, S. Puig, Biomed. J. 36 (2013) 51-58.

[47] S. Erikssons, A. Graslund, S. Skog, L. Thelander, B. Tribukait, J. Biol. Chem. 259 (1984) 11695-11700.

[48] A.M. Florea, D. Büsselberg, Neurotoxicol. 30 (2009) 803-810.

[49] G.R. Ash, F.L. Bygrave, Febs Lett. 78 (1977) 166-168.

[50] O. Mazuryk, O. Krysiak-Foria, A. Żak, F. Suzenet, A. Ptak-Belowska, T. Brzozowski, G. Stochel, M. Brindell, Eur. J. Pharm. Sci. 101 (2017) 43-55.

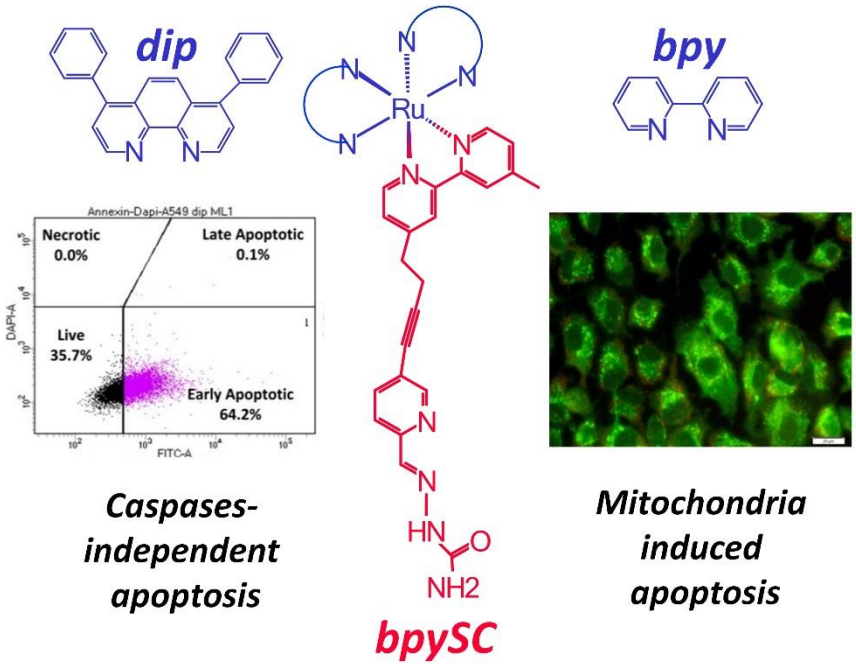

Activity is tuned by auxiliary ligands

Graphical abstract

Appropriately chosen auxiliary ligands can regulate not only cytotoxicity and accumulation of polypyridyl ruthenium complexes, but also determine the mechanism of cellular death and highlight the effects of biologically active molecules.

Highlights

- New Ru complexes with semicarbazone 2-formylopyridine link to bipyridine were synthesised.
- As auxiliary ligands bipyridine and diphenylphenanthroline were chosen.
- The studied compounds were powerful apoptosis inducing agents.
- The anti-proliferative activity was strongly dependent on auxiliary ligands.
- The auxiliary ligands determined effect of the complexes on cell cycle arrest and ROS formation.